



Stewart, J., James, R. H., Anand, P., & Wilson, P. A. (2017). Silicate Weathering and Carbon Cycle Controls on the Oligocene-Miocene Transition Glaciation. *Paleoceanography and Paleoclimatology*.
<https://doi.org/10.1002/2017PA003115>

Publisher's PDF, also known as Version of record

License (if available):
CC BY

Link to published version (if available):
[10.1002/2017PA003115](https://doi.org/10.1002/2017PA003115)

[Link to publication record in Explore Bristol Research](#)
PDF-document

This is the final published version of the article (version of record). It first appeared online via AGU at <http://onlinelibrary.wiley.com/doi/10.1002/2017PA003115/abstract> . Please refer to any applicable terms of use of the publisher.

University of Bristol - Explore Bristol Research

General rights

This document is made available in accordance with publisher policies. Please cite only the published version using the reference above. Full terms of use are available:
<http://www.bristol.ac.uk/red/research-policy/pure/user-guides/ebr-terms/>

RESEARCH ARTICLE

10.1002/2017PA003115

Key Points:

- Foraminiferal Li/Ca suggests that silicate weathering rates increased across the O/M boundary
- High $\delta^{13}\text{C}$ and Cd/Ca during Mi-1 indicate increased primary productivity and nutrient availability
- High U/Ca and low shell weight during Mi-1 suggest increased organic carbon burial

Supporting Information:

- Supporting Information S1
- Table S1

Correspondence to:

J. A. Stewart,
joseph.stewart@bristol.ac.uk

Citation:

Stewart, J. A., James, R. H., Anand, P., & Wilson, P. A. (2017). Silicate weathering and carbon cycle controls on the Oligocene-Miocene transition glaciation. *Paleoceanography*, 32. <https://doi.org/10.1002/2017PA003115>

Received 3 MAR 2017

Accepted 2 OCT 2017

Accepted article online 10 OCT 2017

Silicate Weathering and Carbon Cycle Controls on the Oligocene-Miocene Transition Glaciation

Joseph A. Stewart^{1,2} , Rachael H. James¹ , Pallavi Anand³ , and Paul A. Wilson¹ 
¹National Oceanography Centre Southampton, University of Southampton, Southampton, UK, ²Now at School of Earth Sciences, University of Bristol, Bristol, UK, ³School of Environment, Earth and Ecosystem Sciences, Walton Hall, Open University, Milton Keynes, UK

Abstract Changes in both silicate weathering rates and organic carbon burial have been proposed as drivers of the transient “Mi-1” glaciation event at the Oligocene-Miocene transition (OMT; ~23 Ma). However, detailed geochemical proxy data are required to test these hypotheses. Here we present records of Li/Ca, Mg/Ca, Cd/Ca, U/Ca, $\delta^{18}\text{O}$, $\delta^{13}\text{C}$, and shell weight in planktonic foraminifera from marine sediments spanning the OMT in the equatorial Atlantic Ocean. Li/Ca values increase by 1 $\mu\text{mol/mol}$ across this interval. We interpret this to indicate an ~20% increase in silicate weathering rates, which would have lowered atmospheric CO_2 , potentially forcing the Antarctic glaciation ~23 Ma. $\delta^{13}\text{C}$ of thermocline dwelling planktonic foraminifera track the global increase in seawater $\delta^{13}\text{C}$ across the OMT and during the Mi-1 event, hence supporting a hypothesized global increase in organic carbon burial rates. High $\delta^{13}\text{C}$ previously measured in epipelagic planktonic foraminifera and high Cd/Ca ratios during Mi-1 are interpreted to represent locally enhanced primary productivity, stimulated by increased nutrients supply to surface waters. The fingerprint of high export production and associated organic carbon burial at this site is found in reduced bottom water oxygenation (inferred from high foraminiferal U/Ca) and enhanced respiratory dissolution of carbonates, characterized by reduced foraminiferal shell weight. Replication of our results elsewhere would strengthen the case that weathering-induced CO_2 sequestration preconditioned climate for Antarctic ice sheet growth across the OMT, and increased burial of organic carbon acted as a feedback that intensified cooling at this time.

1. Introduction

The Oligocene-Miocene transition (OMT) at 23 Ma is marked by a rapid (200 kyr) pronounced transient positive excursion ($>1.5\text{‰}$) in the benthic foraminiferal oxygen isotope ($\delta^{18}\text{O}$) record termed the “Mi-1 event” (Figure 1; Miller et al., 1991; Pälike et al., 2006; Paul et al., 2000; Zachos et al., 2001). Ice sheet modeling and reconstructions of deep water temperature suggest that this event represents an interval of temporary ice sheet expansion on Antarctica (to at least present-day Antarctic ice volumes; Gasson et al., 2016; Liebrand et al., 2017, 2011) and cooling of deep waters by approximately 2°C during glacial inception (Lear et al., 2004). The Mi-1 event is also associated with a perturbation of the carbon cycle as indicated by $\delta^{13}\text{C}$ increase in benthic foraminifera (Figure 1; Pälike et al., 2006). While the orbital pacing of this event is now well documented (Liebrand et al., 2017, 2011; Pälike et al., 2006; Zachos et al., 2001), the processes-driving changes in the carbon cycle remain poorly understood.

Global coupled climate-dynamic ice sheet modeling has demonstrated that long-term (10^6 years) decline in atmospheric $p\text{CO}_2$ played an important role in Cenozoic glaciation (DeConto et al., 2008). Processes with the capacity to significantly decrease $p\text{CO}_2$ across the OMT include underlying tectonic drivers, such as increases in global silicate weathering rates (Raymo & Ruddiman, 1992; Walker et al., 1981) as well as short-term feedback mechanisms. These could include a shift in the locus of carbonate burial from the continental shelf to the deep ocean (which may explain carbon cycle changes coupled to Antarctic ice sheet advance at the Eocene-Oligocene transition; Armstrong McKay et al., 2016; Merico et al., 2008) and/or an increase in the ratio of organic carbon to carbonate burial (Florindo et al., 2015; Paul et al., 2000). As yet, however, there is little paleoceanographic geochemical proxy evidence to support any of these mechanisms.

To date, the limited availability of suitable sediment cores and foraminiferal taxonomic ambiguities (Stewart et al., 2012) mean that detailed proxy records for the OMT from both surface and deep water archives remain

©2017. The Authors.

This is an open access article under the terms of the Creative Commons Attribution License, which permits use, distribution and reproduction in any medium, provided the original work is properly cited.

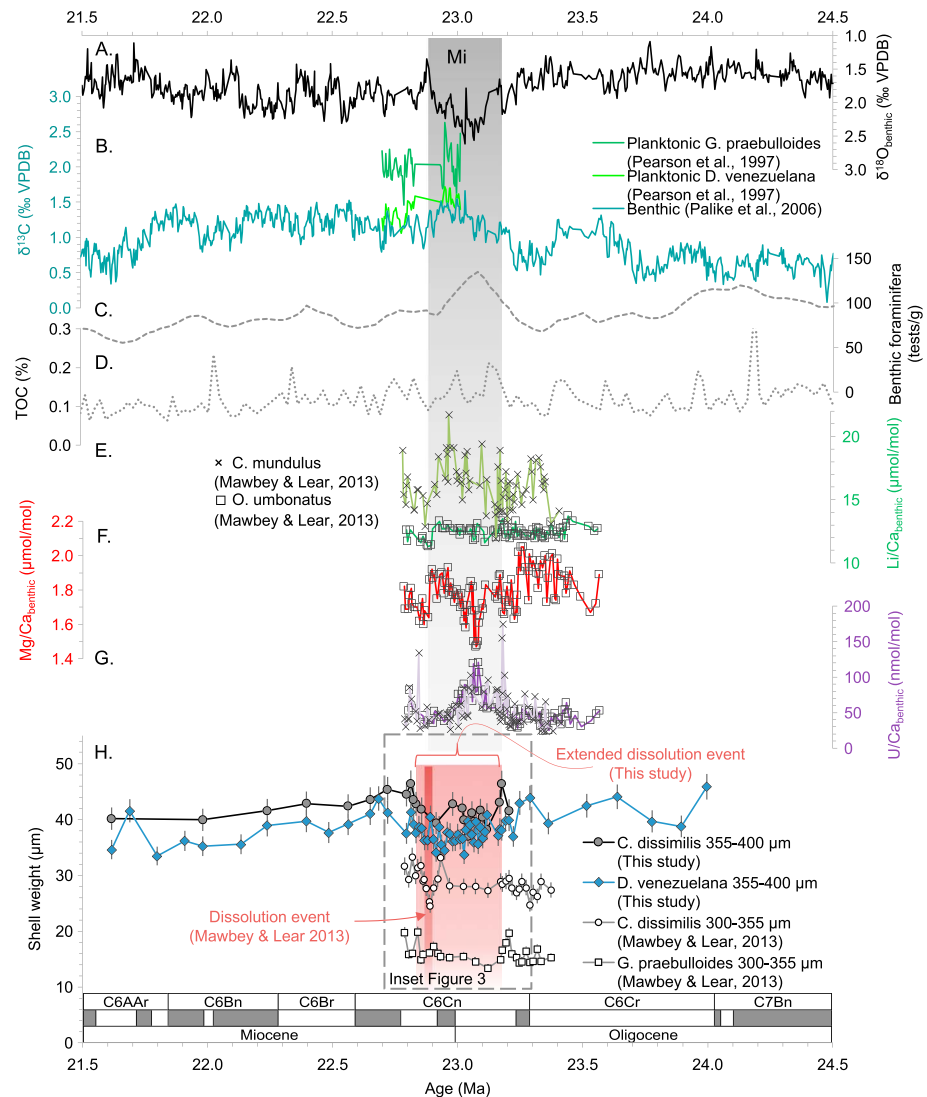


Figure 1. Previous proxy records of carbon cycling and deep water temperature and new planktonic foraminifera shell weight data from ODP site 926 across the OMT. (a, b) Benthic foraminiferal $\delta^{18}\text{O}$ and $\delta^{13}\text{C}$ (Pälike et al., 2006), highlighting the Mi-1 excursion (gray vertical bar). Figure 1b also includes planktonic foraminiferal $\delta^{13}\text{C}$ records from Pearson et al. (1997). (c, d) Benthic foraminiferal tests per gram sediment (5% Gaussian smoothing) and percentage total organic carbon (Diester-Haass et al., 2011). (e–g) Benthic foraminiferal Li/Ca, Mg/Ca and U/Ca records for *C. mundulus* (epifaunal) and *O. umbonatus* (shallow infaunal) (Mawbey & Lear, 2013). (h) Planktonic foraminiferal shell weight records from Mawbey and Lear (2013) and this study. Red vertical bars highlight inferred dissolution intervals.

sparse. Short-term (<800 kyr) benthic foraminiferal Li/Ca, Mg/Ca, and U/Ca and planktonic foraminiferal $\delta^{13}\text{C}$ and $\delta^{18}\text{O}$ records have been generated, respectively, by Mawbey and Lear (2013) and Pearson et al. (1997) (Figure 1). Elevated benthic Li/Ca, low Mg/Ca, and high (>50 nmol/mol) U/Ca during Mi-1 in those records are interpreted to represent cooling of deep water and an increase in bottom water oxygen utilization, perhaps related to enhanced organic carbon burial during the glaciation (Mawbey & Lear, 2013). Planktonic foraminiferal shell weight data from the same study also revealed a brief (<50 kyr) seafloor dissolution event during the glacial recovery, probably caused by enhanced organic matter remineralization (Figure 1; Mawbey & Lear, 2013). However, these records only trace deep water signals and/or span little of the time periods before and after the Mi-1 excursion and hence fail to fully document changes in surface ocean chemistry. To address this gap, we have generated paired shell weight, $\delta^{18}\text{O}$, $\delta^{13}\text{C}$, Li/Ca, Mg/Ca, Cd/Ca, and U/Ca records for planktonic foraminifera recovered from sediments that span the OMT from the equatorial Atlantic Ocean.

2. Methodology

2.1. Proxy Operation

2.1.1. Li/Ca, Mg/Ca, $\delta^{18}\text{O}$, and Shell Weight

The residence time of lithium in the oceans ($\tau_{\text{Li}} \sim 1$ Myr; Huh et al., 1998) is longer than the mixing time of the ocean (1.6 kyr) so the concentration of lithium in seawater ($[\text{Li}]_{\text{sw}}$) is globally uniform (modern $[\text{Li}]_{\text{sw}} = 26 \mu\text{M}$; Morozov, 1968). On timescales greater than τ_{Li} , the rate of change in the amount of lithium in the oceans (M_{Li}) is determined by the balance between the input flux ($F_{\text{Li}}^{\text{Li}}$) of lithium from rivers (RIV; $\sim 8 \times 10^{15}$ mol/Myr at present) and hydrothermal activity (HYD; $\sim 6 \times 10^{15}$ mol/Myr at present) and the output flux to sediments and marine basalts (SED; $\sim 14 \times 10^{15}$ mol/Myr at present) (Hathorne & James, 2006):

$$\frac{\partial M_{\text{Li}}}{\partial t} = F_{\text{RIV}}^{\text{Li}} + F_{\text{HYD}}^{\text{Li}} - F_{\text{SED}}^{\text{Li}} \quad (1)$$

The lithium content of silicate rocks is around 2 orders of magnitude greater than that of carbonates, and field studies show that $>90\%$ of lithium dissolved in rivers is derived from silicate rocks, even in carbonate-dominated catchments, allowing global silicate weathering rates to be constrained from $F_{\text{RIV}}^{\text{Li}}$ (Kisakürek et al., 2005; Vigier et al., 2009). Foraminiferal calcite is an ideal substrate for reconstructing past lithium concentrations of seawater (Delaney et al., 1985); hence, a number of studies have used this technique to reconstruct past variations in silicate weathering rates (Hathorne & James, 2006; Misra & Froelich, 2012). However, interpretation of these data is not straightforward because the Li/Ca ratio of test calcite may be influenced by multiple environmental factors.

The partition coefficient of lithium between calcite and seawater ($D_{\text{Li}} = (\text{Li}/\text{Ca})_{\text{calcite}}/(\text{Li}/\text{Ca})_{\text{sw}}$) is positively correlated with seawater carbonate ion saturation state (defined as $\Omega = [\text{Ca}^{2+}]_{\text{sw}} \times [\text{CO}_3^{2-}]_{\text{sw}} / K_{\text{sp}}^*$), at least in the surface ocean (Hall & Chan, 2004). Yet D_{Li} also shows an inverse relationship with calcification temperature (Marriott et al., 2004). Thus, these two hydrographic variables serve to, respectively, increase and decrease the resultant Li/Ca ratio of planktonic foraminifera. Consequently, an abrupt decrease (by $\sim 30\%$) is documented in planktonic foraminiferal Li/Ca during the last deglaciation (~ 12 ka) as the oceans warmed and Ω fell (Burton & Vance, 2000; Hall & Chan, 2004; Hall et al., 2005). To reconstruct changes in $[\text{Li}]_{\text{sw}}$ from Li/Ca of ancient planktonic foraminifera, independent proxies for surface water Ω and temperature are therefore required. Here we use the planktonic foraminiferal proxies of shell weight (Barker & Elderfield, 2002; Beer et al., 2010b; Broecker & Clark, 2001) combined with $\delta^{18}\text{O}$ (Bemis et al., 1998) and Mg/Ca (Anand et al., 2003) to assess the respective effects of Ω and temperature on our Li/Ca data.

2.1.2. Organic Carbon Cycling

Organic carbon content in marine sediments is controlled by the rate of export production from the surface ocean, sedimentation rates, and postdepositional remineralization (Tyson, 2001). Slightly elevated total organic carbon concentrations at Site 926 during Mi-1 therefore potentially indicate enhanced productivity (Figure 1; Diester-Haass et al., 2011), but proxies for organic matter export production and surface water nutrient availability are required to test this hypothesis.

$\delta^{13}\text{C}$ values of nonphotosymbiont-bearing planktonic foraminifera are strongly influenced by the $\delta^{13}\text{C}$ value of dissolved inorganic carbon ($\delta^{13}\text{C}_{\text{DIC}}$) in surface waters. Surface water $\delta^{13}\text{C}_{\text{DIC}}$ can be altered by a number of processes including (i) weathering of (typically ^{12}C depleted) shallow water carbonates (e.g., through glacioeustatic exposure; Merico et al., 2008), (ii) upwelling of ^{12}C -enriched deep waters, or (iii) increased export production that preferentially removes ^{12}C from surface waters (Kroopnick, 1985). This latter control means that $\delta^{13}\text{C}$ in planktonic foraminiferal calcite provides a means to assess changes in primary productivity in surface waters.

The distribution of cadmium in the world oceans strongly resembles that of the labile nutrient phosphate (Boyle et al., 1976), so the Cd/Ca ratio of foraminiferal calcite has been used as a paleonutrient tracer (Rickaby & Elderfield, 1999; Rosenthal et al., 1997). Estimates of the concentration of phosphate in ambient seawater ($[\text{PO}_4]_{\text{sw}}$) can be made from Cd/Ca ratios in foraminiferal calcite ($(\text{Cd}/\text{Ca})_{\text{foram}}$) (de Baar et al., 1994; Rickaby & Elderfield, 1999):

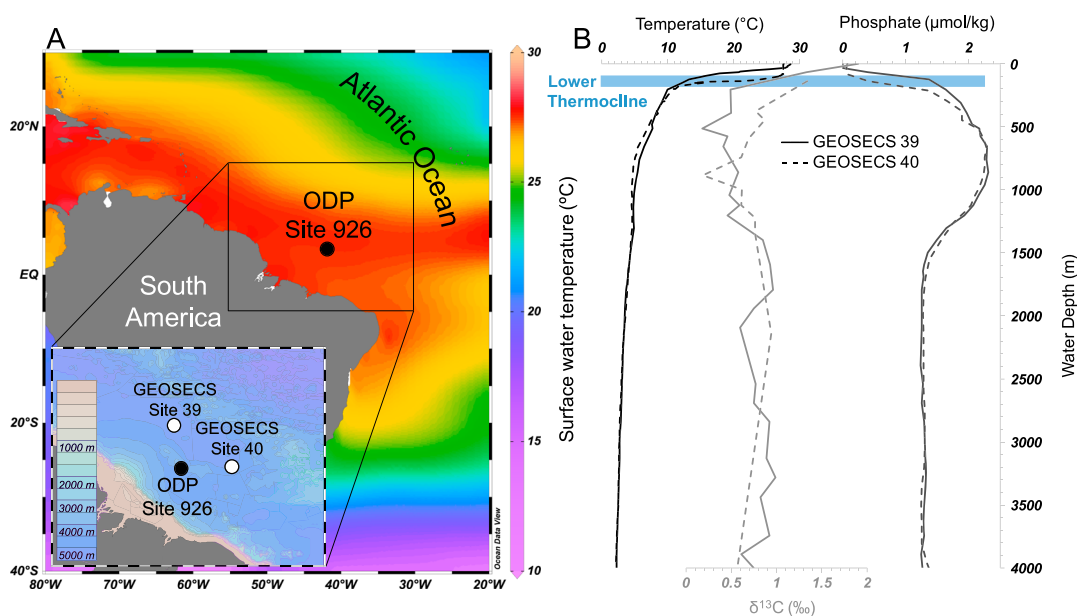


Figure 2. Location and modern hydrography of ODP Site 926 on Ceara Rise. (a) Average surface water temperature (Locarnini et al., 2013) and bathymetry of study site (inset). (b) Temperature, carbon isotope, and phosphate profiles measured at GEOSECS sites proximal to Ceara Rise (Bainbridge, 1980).

$$[\text{PO}_4]_{\text{sw}} = \frac{(\text{Cd}/\text{Ca})_{\text{foram}} \times [\text{Ca}^{2+}]_{\text{sw}}}{D_{\text{Cd}} \times (\text{Cd}/\text{P})_{\text{sw}}} \quad (2)$$

where $(\text{Cd}/\text{P})_{\text{sw}}$ and $[\text{Ca}]_{\text{sw}}$ are, respectively, the Cd/P ratio and calcium concentration of seawater. In this way, the Cd/Ca ratio of planktonic foraminiferal calcite can be used to assess surface water nutrient concentrations. While the factors controlling export production at a particular site are complex (Arndt et al., 2013; Henson et al., 2012), intervals of increased nutrient availability at oligotrophic sites such as Ceara Rise may facilitate higher primary productivity, promoting export of organic carbon to the deep ocean (Howarth, 1988).

In contrast to Li/Ca, Mg/Ca, and Cd/Ca ratios in planktonic foraminifera, U/Ca values are highly susceptible to postdepositional alteration if the oxygen concentration in pore fluids or overlying bottom water is low (Mangini et al., 2001; Russell et al., 1996, 2004). In these circumstances, planktonic foraminiferal U/Ca values are very high (>10 nmol/mol) and are often associated with high Mn/Ca (>100 μmol/mol; Lea et al., 2005; Mangini et al., 2001; Russell et al., 1996). Elevated U/Ca ratios in foraminifera therefore provide evidence for increased oxygen consumption (Algeo & Rowe, 2012), which is linked to the flux of organic carbon that reaches the seafloor (Smith & Baldwin, 1984).

2.2. Geological Setting and Chronology

Sediment samples spanning the OMT were collected from Ocean Drilling Program (ODP), Leg 154 Site 926 Hole B (Figure 2; 3°43.148'N, 42°54.507'W, 3,598 m present water depth; Shipboard Scientific Party, 1995) between 428.02 and 491.19 m below seafloor. Magnetostratigraphic age control is not available at Ceara Rise drill sites, but a high-quality magnetostratigraphy is available for ODP Site 1090 on the Agulhas Ridge (Channell et al., 2003), and this has been correlated to Site 926 (Liebrand et al., 2011). Sample ages given in our study are reported using the astronomically tuned age model of ODP Site 926 (Pälike et al., 2006). Sediment samples of 30 cm³ were taken at every ~2.5 m (~100 kyr spacing), increasing to every 30 cm (~10 kyr) across the benthic δ¹⁸O maximum to capture any high-frequency geochemical variability associated with the Mi-1 event.

2.3. Sample Preparation and Analysis of Shell Weight

Sediment samples were dried in an oven at 50°C, weighed, then gently disaggregated in deionized water and washed over a 63 μm sieve. Sediment retained in the sieve was reweighed to calculate the percentage coarse

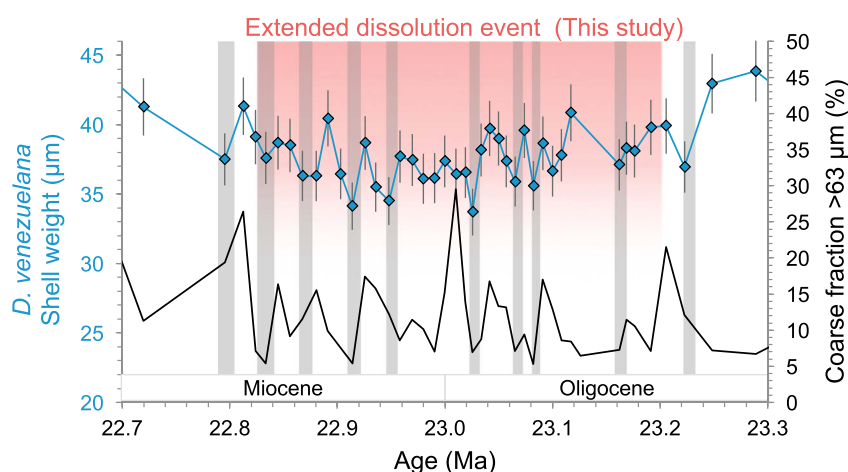


Figure 3. High-resolution interval of *D. venezuelana* shell weight record during the peak Mi-1 compared to percentage coarse fraction data (this study). Red vertical bar shows inferred 400 kyr extended dissolution interval, and gray bars show shell weight minima.

fraction ($>63 \mu\text{m}$) of dry sediment (supporting information Table S1). Approximately 1 mg of the large, abundant, and continuously present planktonic foraminifera *Dentoglobigerina venezuelana* was picked from the 355–400 μm size fraction for trace element analysis. Mg/Ca, $\delta^{18}\text{O}$, and $\delta^{13}\text{C}$ data from nearby ODP Site 925 reveal that large *D. venezuelana* specimens ($>355 \mu\text{m}$) were nonphotosymbiont bearing and inhabited the same thermocline depth habitat at Ceara Rise throughout this interval (Stewart et al., 2012). A further 10 individual *D. venezuelana* specimens were picked from the 300–355 μm size fraction of each sample for stable oxygen and carbon isotope analysis.

Prior to cleaning, subsamples of 20 individual tests (355–400 μm) of *D. venezuelana* and a second species *Catapsydrax dissimilis* (subthermocline dweller; Stewart et al., 2012) were weighed using a microbalance to determine the average size-normalized shell weight of each species. For this study, we adopted the simple “sieve-based weight” technique (estimated accuracy $\pm 11\%$; Beer et al., 2010a). Adhering clay particles were removed by ultrasonication in deionized water and methanol. Samples were then subject to first reductive then oxidative cleaning to remove ferromanganese oxide coatings and organic matter, respectively. Finally, the tests were leached in weak acid (0.001 M HNO_3) (Boyle & Keigwin, 1985). Once cleaned, samples were dissolved in 0.075 M HNO_3 .

2.4. Analytical Techniques

2.4.1. Stable Isotope Analysis

D. venezuelana samples were gently crushed and ultrasonicated in deionized water before approximately 200 μg of material was taken for $\delta^{13}\text{C}$ and $\delta^{18}\text{O}$ analysis using a Thermo Scientific Kiel IV Carbonate device coupled with a MAT253 isotope ratio mass spectrometer at the University of Southampton. Results are presented in delta notation as the per mil variation from Vienna Pee Dee Belemnite. Replicate analyses of an in-house standard are calibrated to NBS-18 and yield a reproducibility of $\pm 0.05\text{‰}$ for $\delta^{18}\text{O}$ and $\pm 0.04\text{‰}$ for $\delta^{13}\text{C}$ (1σ).

2.4.2. Trace Element Analysis

Prior to trace element analysis, the Ca contents of dissolved samples were assessed using a Perkin-Elmer Optima 4300 DV inductively coupled plasma optical emission spectrometer (Green et al., 2003). Sample aliquots were then diluted to give 100 ppm of Ca. Solutions were analyzed using a Perkin Elmer Elan DRC II ICP mass spectrometer, calibrated using matrix-matched synthetic standard solutions, to give Li/Ca, Mg/Ca, Cd/Ca, and U/Ca ratios following Rosenthal et al. (1999). Al/Ca and Mn/Ca ratios were also determined to test the efficacy, respectively, of clay mineral and ferromanganese coating removal. Only samples with Al/Ca ratios $<200 \mu\text{mol/mol}$ after cleaning were deemed to be unaffected by clay contamination and considered in subsequent discussions. The external reproducibility of trace element ratios was calculated from repeat measurements of two foraminiferal calcite consistency standards ($n = 23$, for each standard) yielding the

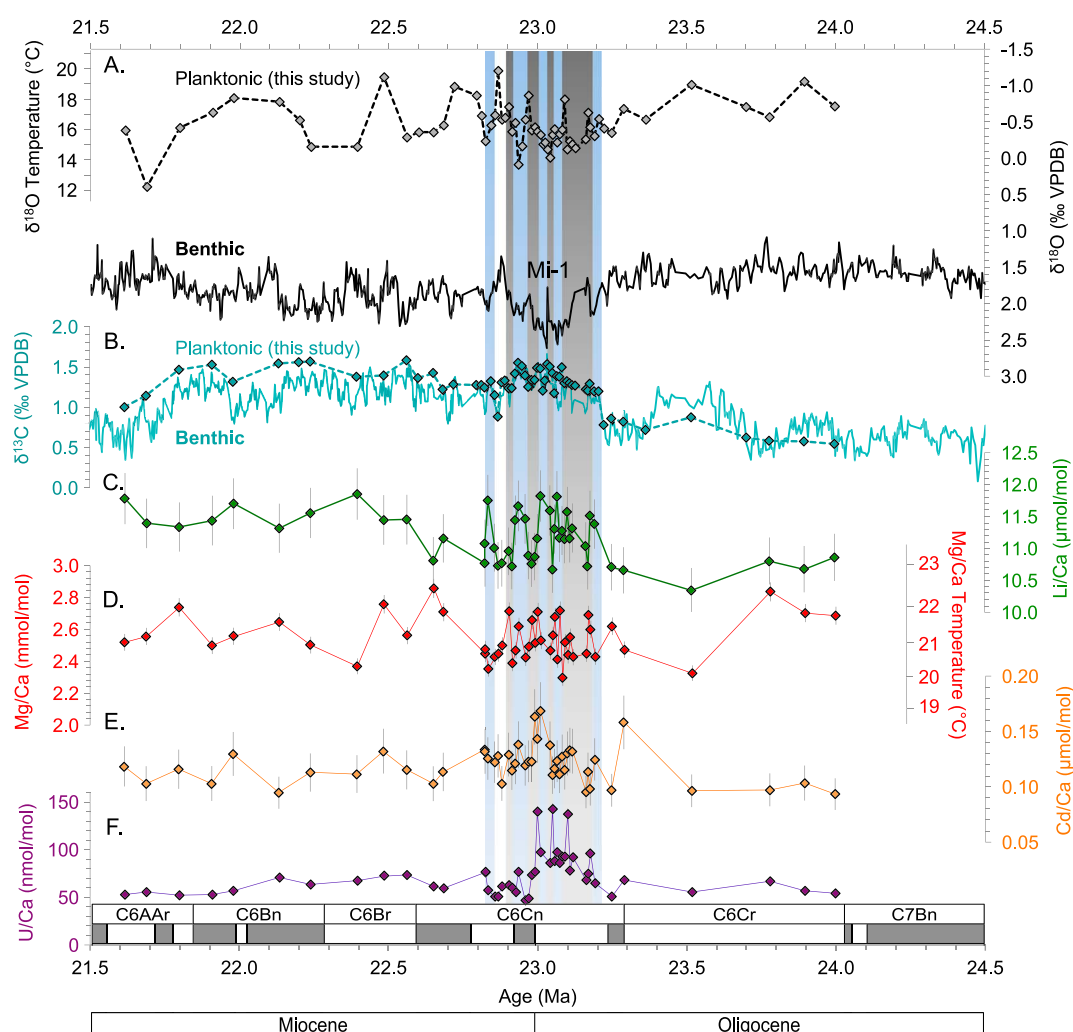


Figure 4. Planktonic foraminiferal trace element and isotopic records from ODP Site 926. (a, b) *D. venezuelana* (this study) and benthic (Pälike et al., 2006) foraminiferal $\delta^{18}\text{O}$ (scale inverted) and $\delta^{13}\text{C}$. Gray vertical bar highlights Mi-1 event, and blue narrow bars show short-term (<100 kyr) benthic $\delta^{18}\text{O}$ maxima during the O/M interval. (c–f) Records of Li/Ca, Mg/Ca, Cd/Ca, and U/Ca measured in *D. venezuelana*. Mg/Ca and $\delta^{18}\text{O}$ temperature scales based on Anand et al. (2003) and Bemis et al. (1998) (see text). Error bars represent 2σ external reproducibility.

following 2σ uncertainties: Li/Ca $\pm 3.4\%$, Mg/Ca $\pm 2.1\%$, Al/Ca $\pm 11.8\%$, Mn/Ca $\pm 6.9\%$, Cd/Ca $\pm 15.3\%$, and U/Ca $\pm 4.1\%$.

3. Results

The average shell weight of both *D. venezuelana* and *C. dissimilis* is approximately 40 μg over the interval of study (between 24 and 21.5 Ma). The two species exhibit similar variations in shell weight over time with a broad minimum of 35 μg associated with the benthic foraminiferal $\delta^{18}\text{O}$ maximum during the Mi-1 event at 23 Ma (Figure 1h). This minimum is bounded by shell weight maxima (45 μg) approximately 200 kyr either side of Mi-1. In addition, *D. venezuelana* shows a long-term decrease in shell weight, of between 5 and 10 μg , across the entire interval. In detail (Figure 3), high-frequency (<100 kyr) shell weight minima that contribute to the broad low in *D. venezuelana* shell weight during the Mi-1 event correspond to low percentage coarse fraction.

We compare our planktonic foraminiferal stable isotope and trace element data generated from the OMT interval of ODP Site 926 (Figure 4) with the benthic foraminiferal $\delta^{18}\text{O}$ and $\delta^{13}\text{C}$ records (plots A and B) for this site (Pälike et al., 2006). $\delta^{18}\text{O}$ values for *D. venezuelana* are around 2‰ lower than corresponding benthic values. Planktonic $\delta^{18}\text{O}$ increases very slightly (by $\sim 0.5\text{‰}$) between 24 and 21.5 Ma, punctuated by a small

(+0.5‰) transient (500 kyr) increase during the Mi-1 event at 23 Ma (vertical gray bar). Planktonic foraminiferal $\delta^{13}\text{C}$ values also increase over between 24 and 21.5 Ma (by almost 1‰) and also increase sharply (by >0.5‰) during the Mi-1 event. The $\delta^{13}\text{C}$ values that we measure for *D. venezuelana* are similar to those reported by Pearson et al. (1997) (Figure 1) and show close resemblance to values observed in contemporaneous benthic foraminiferal calcite (Pälike et al., 2006).

Li/Ca in *D. venezuelana* also shows an overall increase from 10.5 $\mu\text{mol/mol}$ in the late Oligocene (~24 Ma) to 11.5 $\mu\text{mol/mol}$ in the early Miocene (~22 Ma; Figure 4c). This trend is again punctuated by a transient increase of >0.5 $\mu\text{mol/mol}$ during the Mi-1 event, which is composed of higher-frequency oscillations (<100 kyr) of high Li/Ca that coincide with benthic foraminiferal $\delta^{18}\text{O}$ maxima at 22.83, 22.93, 23.02, 23.06, 23.10, and 23.19 Ma (blue vertical bars). The mean Mg/Ca value measured in *D. venezuelana* is approximately 2.5 mmol/mol (Figure 4d); however, unlike Li/Ca, Mg/Ca shows no long-term or systematic change across the interval between 24.0 and 21.5 Ma.

Except for one sample at 23.3 Ma, Cd/Ca values in *D. venezuelana* are relatively constant (~0.1 $\mu\text{mol/mol}$) in the runup to the OMT (Figure 4e). However, Cd/Ca values increase to a well-defined short maximum of ~0.15 $\mu\text{mol/mol}$ between 23.2 and 22.8 Ma, during the peak of the Mi-1 glaciation. Similarly, U/Ca values are relatively stable (~70 nmol/mol) before and after the OMT but show a broad maximum (>120 nmol/mol) during the Mi-1 event (Figure 4f). The highest U/Ca values, however, do not coincide perfectly with the highest benthic $\delta^{18}\text{O}$ values; rather, U/Ca returns to low, preexcursion, values ~100 kyr before the termination of the Mi-1 event. This is in contrast to our other trace element records that exhibit excursions that persist throughout the 200 kyr Mi-1 event.

The Mn/Ca ratio of cleaned planktonic foraminiferal calcite in this study ranges from 500 to 1,000 $\mu\text{mol/mol}$. These values are high, but we find no correlation ($R^2 \sim 0$) between Mn/Ca measured in our planktonic foraminiferal calcite samples and Li/Ca, Cd/Ca, or Mg/Ca suggesting that these Mn-rich phases have little overall effect on trace element compositions.

4. Discussion

4.1. Saturation State of Seawater

Calcium isotope measurements of planktonic foraminiferal calcite indicate that $[\text{Ca}]_{\text{sw}}$ remained near constant between 25 and 20 Ma (Heuser et al., 2005); hence, changes in the saturation state of seawater at Ceara Rise during the OMT were primarily driven by $[\text{CO}_3^{2-}]$. Ceara Rise was bathed in oligotrophic waters throughout the Cenozoic (Shipboard Scientific Party, 1995); thus, it is reasonable to infer that, to a first order, saturation states of surface and thermocline waters at Site 926 were closely coupled, permitting changes in surface water saturation state to be estimated from our thermocline dwelling foraminifera.

Using the relationship between Ω and shell weight of Broecker and Clark (2001) and Barker and Elderfield (2002), our shell weight data might be taken to suggest that the $[\text{CO}_3^{2-}]$ of thermocline waters decreased gradually between 24 and 21.5 Ma, with a more abrupt decrease of between 30 and 60 $\mu\text{mol/kg}$ at the peak of the Mi-1 event. However, shell weight minima during Mi-1 in our records are associated with minima in the sand fraction record (Figure 3) suggesting that tests deposited at the peak of the Mi-1 event were affected by dissolution in the water column or on the seafloor. While records from other sites are required to rule out a change in ocean circulation resulting in the delivery of low pH deep waters to Ceara Rise, release of metabolic CO_2 from organic matter remineralization within the sediments is a likely cause of dissolution (Hales & Emerson, 1997). Our shell weight data may imply that export of organic carbon increased during the Mi-1 event, possibly as a result of increased primary production at Ceara Rise (see section 1). This interpretation is consistent with that of Mawbey and Lear (2013), who document a brief (100 kyr duration) reduction in *C. dissimilis* shell weight during Mi-1 at this site, although our records are in detail more similar to the *Globigerina praebulloides* shell weight record (Figure 1h). Our shell weight records span a broader interval and suggest that the imprint of marked seafloor carbonate dissolution persisted longer (~400 kyr duration).

4.2. Preservation of Primary Test Chemistry

A reduction in foraminiferal $\delta^{13}\text{C}$ and Mg/Ca values together with an increase in and increasing of $\delta^{18}\text{O}$ is often observed during partial dissolution of test calcite (Lohmann, 1995; Rosenthal & Lohmann, 2002).

Table 1

Literature Values for Partition Coefficients of Trace Elements ($D_X = (X/Ca)_{\text{calcite}}/(X/Ca)_{\text{sw}}$) Into Inorganic and Foraminiferal Calcite

	D_{Li}	D_{Mg}	D_{Cd}	D_{U}
Inorganic calcite	2×10^{-3}	2×10^{-2}	$2 \times 10^{+1}$	2×10^{-1}
Planktonic foram calcite	5×10^{-3}	6×10^{-4}	3×10^0	7×10^{-3}
Benthic foram calcite	7×10^{-3}	6×10^{-4}	2×10^0	2×10^{-2}

Note. Data from D_{Li} (Delaney et al., 1985; Hathorne & James, 2006; Marriott, Henderson, Belshaw, et al., 2004; Marriott, Henderson, Crompton, et al., 2004), D_{Mg} (Anand et al., 2003; Baker et al., 1982; Dekens et al., 2002; Lea et al., 2000; Sexton et al., 2006), D_{Cd} (Delaney, 1989; Havach et al., 2001; Lorens, 1981; Mashiotta et al., 1997; McCorkle et al., 1995; Ripperger et al., 2008; Rosenthal et al., 1997), and D_{U} (Meece & Benninger, 1993; Russell et al., 1994, 2004).

These dissolution effects must therefore be considered when interpreting stable isotope and trace element proxy data within the inferred dissolution event at this site during Mi-1. However, the taphonomy of all planktonic foraminifera used in this study is “frosty” rather than “glassy” (e.g., Sexton et al., 2006) indicating that all samples analyzed here, throughout the OMT, have undergone some degree of recrystallization. Below we discuss the implications of this on the interpretation of our records, particularly where trace metal partition coefficients (D) between inorganic calcite and seawater, and biogenic calcite and seawater, are different (Table 1).

$\delta^{18}\text{O}$ in planktonic foraminiferal calcite is susceptible to alteration by calcite recrystallization in cold deep waters on the seafloor. This process leads to underestimation of surface ocean temperatures meaning that

relative changes in temperature are more reliable than absolute values (Sexton et al., 2006). $\delta^{13}\text{C}_{\text{DIC}}$ that generally decreases with water depth as organic matter, enriched in ^{12}C , is removed from the surface ocean by primary production and remineralized at depth (Figure 2b). The resulting planktonic-benthic gradient in $\delta^{13}\text{C}$ is small, however, so primary $\delta^{13}\text{C}$ values in planktonics are robust to seafloor recrystallization.

D_{Li} for foraminiferal calcite is similar to D_{Li} in inorganic calcite, whereas D_{Mg} for inorganic calcite precipitated in laboratory experiments may be up to 2 orders of magnitude greater than that of biogenic calcite (e.g., inorganic calcite $D_{\text{Mg}} = 0.06$ to 0.02 ; Katz, 1973; Sexton et al., 2006). However, deep water diagenetic carbonates have much lower D_{Mg} ($D_{\text{Mg}} = 8.1 \times 10^{-4}$; Baker et al., 1982), closer to the value for biogenic calcite (Sexton et al., 2006). Similarity between biogenic and inorganic calcite partition coefficients implies that the contribution of recrystallization to test Li/Ca and Mg/Ca is likely to be small in a carbonate-rich closed system, such as Ceara Rise. Mg/Ca-based temperature estimates are therefore expected to be more reliable than planktonic $\delta^{18}\text{O}$; however, the temperature dependency of D_{Mg} (Anand et al., 2003) dictates that Mg/Ca in specimens recrystallized in the cold deep ocean must be interpreted with some caution.

By contrast, the partition coefficients for Cd and U into inorganic calcite are, respectively, 1 and 2 orders of magnitude greater than they are for planktonic foraminiferal calcite. The U/Ca ratio of the foraminiferal test is therefore susceptible to overprinting by the addition of inorganic calcite during test recrystallization. The extremely high U/Ca values measured in planktonic foraminifera in this study (>40 nmol/mol) relative to core top and plankton tow samples from Ceara Rise (10 nmol/mol; Russell et al., 1994) suggest that U in our samples is chiefly present in diagenetic calcite (e.g., Lea et al., 2005; Mangini et al., 2001; Russell et al., 1996). The influence of diagenesis on the Cd/Ca ratio of our samples, however, is less clear. The Cd/Ca ratio of uncleaned planktonic foraminiferal calcite is generally >1 $\mu\text{mol/mol}$ (Boyle, 1981), whereas cleaned planktonic foraminifera commonly have Cd/Ca ratios of <0.1 $\mu\text{mol/mol}$ (Rickaby & Elderfield, 1999). Enrichment of Cd in uncleaned foraminifera may result from recrystallization (D_{Cd} of inorganic calcite is high; Table 1) or incorporation of pore water Cd in Fe-Mn coatings (Tachikawa & Elderfield, 2002). Cd/Ca values measured in this study are, however, similar to North Atlantic core top measurements for *Globorotalia truncatulinoides* (which is also deeper-thermocline dwelling; Cd/Ca = 0.08 $\mu\text{mol/mol}$; Ripperger et al., 2008). This perhaps suggests that our Cd/Ca values are minimally affected by diagenesis although we acknowledge that overprinting of the primary surface water Cd/Ca signal cannot be fully discounted.

4.3. Seawater Temperature

Changes in thermocline temperature can be assessed using our planktonic foraminiferal $\delta^{18}\text{O}$ and Mg/Ca data. To this end, we apply the temperature calibrations for modern *Orbulina universa* from Bemis et al. (1998)

$$T (^{\circ}\text{C}) = 16.5 - 4.8 (\delta^{18}\text{O}_{\text{foram}} - \delta^{18}\text{O}_{\text{seawater}}) \quad (3)$$

and the “all planktonic species” Mg/Ca temperature calibration of Anand et al. (2003)

$$\text{Mg/Ca}_{\text{foram}} = 0.38 \exp(0.090 \times T) \quad (4)$$

The $\delta^{18}\text{O}$ value of seawater varies as a function of salinity and global ice volume. Although unlikely to be constant, for simplicity, the $\delta^{18}\text{O}$ value of seawater for late Oligocene in equation (3) is considered to be -0.5‰

throughout the OMT (Lear et al., 2004). Similarly, we also assume that the Mg/Ca value of seawater was the same as the present day and remained unchanged during the OMT. In this way, our data indicate that absolute thermocline temperatures based on Mg/Ca are more than 3°C higher than those estimated using planktonic $\delta^{18}\text{O}$ (Figures 4a and 4d). This is not unexpected because planktonic foraminiferal $\delta^{18}\text{O}$ is more susceptible to alteration during calcite recrystallization. Use of an alternative planktonic foraminiferal $\delta^{18}\text{O}$ -temperature calibration (e.g., *G. bulloides*; Bemis et al., 2000) and/or adjustment of the preexponent of the Mg/Ca-temperature calibration to account for seawater Mg/Ca ratios lower than present day during the OMT (Lear, Elderfield, & Wilson, 2000) serve to increase the discrepancy between the two proxies.

Nevertheless, our Mg/Ca data suggest that Ceara Rise thermocline temperatures varied by less than 3°C across the interval, and there was no reduction in thermocline temperature at this location during the Mi-1 event. This result is even consistent with our (arguably less reliable) planktonic $\delta^{18}\text{O}$ temperature estimates that suggest cooling between 24 and 21.5 Ma and during the Mi-1 event that was restricted to less than 2°C. Furthermore, if the reduction in shell weight during Mi-1 is primarily driven by dissolution, then application of a dissolution-adjusted Mg/Ca (Rosenthal & Lohmann, 2002) and $\delta^{18}\text{O}$ (Lohmann, 1995) temperature calibration further rule out any cooling, serving to slightly increase thermocline temperature estimates (by ~1°C) during the Mi-1 event.

4.4. Environmental Controls on Foraminiferal Li/Ca on Short (<1 Myr) Timescales

The changes in the Li/Ca ratio of planktonic foraminifera at Ceara Rise during the 200 kyr excursion at Mi-1 (Figure 4c) cannot be a result of changes in $[\text{Li}]_{\text{sw}}$ because τ_{Li} is long (~1 Myr). Rather, these rapid changes in planktonic foraminiferal Li/Ca during the Mi-1 event are in step with higher-frequency benthic $\delta^{18}\text{O}$ variability (Figure 4c; vertical blue bars), suggesting that the Li/Ca ratio of *D. venezuelana* varies as a function of calcification temperature and/or Ω . Li/Ca measurements in modern foraminifera in the North Atlantic indicate a temperature sensitivity of ~ -1.5% per °C (Hathorne & James, 2006). Assuming a similar temperature sensitivity and no other controls, our data would require a large (6°C) reduction in thermocline temperatures during the Mi-1 event. Alternatively, if Li/Ca was controlled by changes in carbonate chemistry alone, then, using the relationships determined by Hall and Chan (2004), this change in Li/Ca corresponds to an increase in thermocline $[\text{CO}_3^{2-}]$ of 20 $\mu\text{mol/kg}$ to a value that is about 10% higher than the modern value (Takahashi et al., 1981).

Our Mg/Ca and $\delta^{18}\text{O}$ data do not support a significant decrease in thermocline temperature during the Mi-1 event; hence, the contemporaneous increase in Li/Ca (as well as the higher-frequency glacial maxima) is more likely attributed to an increase in Ω of thermocline waters. This hypothesis is consistent with modeling results of other intervals of rapid continental ice sheet growth (and thus sea level lowering) during the Oligocene (Armstrong McKay et al., 2016; Merico et al., 2008) where exposure of shelf carbonates reduced carbonate burial and increased the carbonate weathering flux to the ocean. This combination would increase Ω of seawater.

4.5. Controls on Foraminiferal Li/Ca Over Long (>1 Myr) Timescales

We reason that changes in planktonic foraminiferal Li/Ca on timescales shorter than τ_{Li} are predominantly controlled by seawater Ω . By contrast, the longer-term ~1 $\mu\text{mol/mol}$ increase in Li/Ca between 24 Ma and 21.5 Ma might be attributed to (i) decreasing thermocline temperature, (ii) an increase in the Ω of seawater, (iii) a decrease in $[\text{Ca}]_{\text{sw}}$ of ~1 mmol/kg (impacting both Li/Ca ratio of seawater and potentially carbonate ion concentration; Hain et al., 2015), and/or (iv) an increase in $[\text{Li}]_{\text{sw}}$. The first three of these scenarios are, however, unlikely.

1. Benthic foraminiferal $\delta^{18}\text{O}$ records show that the main climate signal across this interval was a transient glaciation (Pälike et al., 2006; Zachos et al., 2001). Furthermore, *D. venezuelana* Mg/Ca and $\delta^{18}\text{O}$ values imply that there was little variation in thermocline temperature at Ceara Rise during the OMT, suggesting that temperature is unlikely to have driven the observed increase in Li/Ca.
2. There is no evidence for permanent deepening of the carbonate compensation depth at the OMT (Pälike et al., 2012), and the overall decrease in planktonic foraminiferal shell weight suggests that thermocline $[\text{CO}_3^{2-}]$ may have actually decreased across the OMT (serving to decrease planktonic foraminiferal Li/Ca). This interpretation assumes that, unlike during the peak Mi-1 event, our foraminiferal shell weight records either side of the glacial interval are not severely influenced by dissolution.

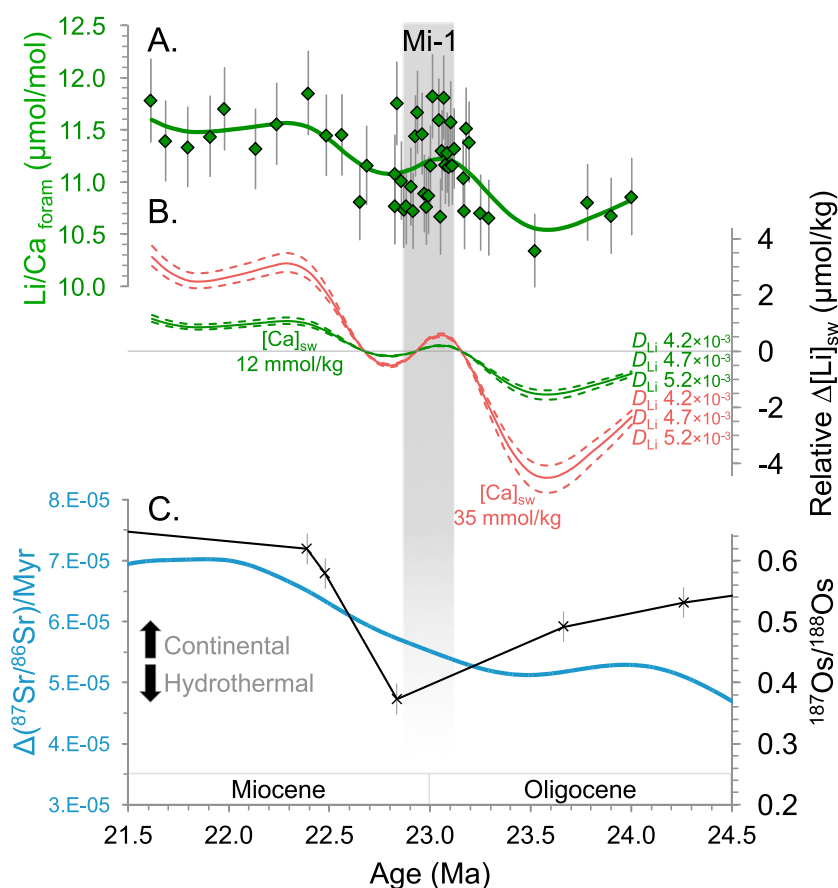


Figure 5. (a) Smoothed fit to Li/Ca ratios for *D. venezuelana* ("smoother" tool JMP software 9.0). (b) Reconstructions of the relative change in $[Li]_{sw}$ from smoothed Li/Ca_{foram} data for various $[Ca]_{sw}$ and D_{Li} (see text for details). (c) Seawater osmium (Peucker-Ehrenbrink & Ravizza, 2000) and strontium (McArthur, 2004) isotope records, for comparison. Sr isotope data are shown as the rate of change of seawater $^{87}Sr/^{86}Sr$ and show that OMT is characterized by a more rapid increase in weathering rate relative to the early Oligocene and late Miocene.

3. Calcium isotope measurements suggest that $[Ca]_{sw}$ was relatively constant between 25 and 20 Ma (~12 mmol/kg; Heuser et al., 2005), although other studies (Griffith et al., 2008; Hardie, 1996) suggest that it may be more variable (see below). Nevertheless, our other trace element records, also normalized to Ca, do not show any increase between ~24 Ma and ~21.5 Ma, further implying that a large decrease in $[Ca]_{sw}$ is unlikely. We conclude that the long-term change in Li/Ca of planktonic foraminiferal calcite is due to an increase in $[Li]_{sw}$ over this 2.5 Myr interval.

To quantify the magnitude of secular change in $[Li]_{sw}$ required to explain our Li/Ca record, we begin by smoothing the Li/Ca record of *D. venezuelana* (Figure 5). We make various estimates of the relative change (Δ) in $[Li]_{sw}$ for differing values of D_{Li} (based on measurements of modern planktonic foraminifera; Delaney et al., 1985; Hathorne & James, 2006) and $[Ca]_{sw}$ during the O/M interval. $[Ca]_{sw}$ at the OMT is assumed to lie between ~12 mmol/kg (Heuser et al., 2005) and ~35 mmol/kg (Hardie, 1996) (note that the latter value is more than 3 times greater than modern $[Ca]_{sw}$ = 10 mmol/kg). Reconstructed $\Delta[Li]_{sw}$ is highly sensitive to our choice of $[Ca]_{sw}$ (Figure 5). If $[Ca]_{sw}$ = 12 mmol/kg, then the $[Li]_{sw}$ was close to that of the modern ocean (26 μmol/kg; M_{Li} 3.5×10^{16} mol; Morozov, 1968) and $[Li]_{sw}$ is estimated to have increased by ~2 μmol/kg (an increase in M_{Li} of 3.6×10^{15} mol) across this interval. If the higher value for $[Ca]_{sw}$ is used, then $[Li]_{sw}$ increased by >6 μmol/kg.

An increase in $[Li]_{sw}$ of 2 μmol/kg requires a change in the flux of lithium to/from the oceans (equation (1); Hathorne & James, 2006). Oceanic crustal production rates remained relatively constant over this interval (Rowley, 2002) so large changes in hydrothermal inputs of lithium or removal into marine sediments are unlikely (Hathorne & James, 2006). Furthermore, the lithium isotopic composition of seawater, inferred from

foraminiferal $\delta^7\text{Li}$, shows little change across this interval ($<2\text{‰}$ between 30 and 20 Ma; Misra & Froelich, 2012), implying that the proportion of lithium retained in secondary clay minerals (which preferentially incorporate ^6Li ; Huh et al., 1998) was unchanged throughout this interval. The best explanation for higher $[\text{Li}]_{\text{sw}}$ is therefore increased delivery of lithium down rivers through higher silicate weathering rates.

The flux of lithium from rivers required to increase M_{Li} by 3.6×10^{15} mol in 2 Myr is 9.8×10^{15} mol/Myr, approximately 20% higher than today's value. Assuming that riverine lithium is predominantly derived from weathering of silicate rocks of similar lithium content (Kisakürek et al., 2005), this represents a substantial increase in the overall global silicate weathering rate. Although approximately half of this increase appears to occur after the inception of the Mi-1 (note that the timing of Li/Ca change is dependent on the robustness of the smoothing function in Figure 5a), the large increase in silicate weathering rate could act to lower $p\text{CO}_2$, perhaps forcing the glacial expansion at 23 Ma.

Currently, the Earth is considered to be in a “reaction-limited” weathering regime, in which the supply of freshly eroded rock is plentiful (Stallard & Edmond, 1983). In a warmer, more “transport-limited” early ice-house world silicate weathering rates are expected to have responded more strongly to the generation of fresh easily weathered material exposed through orogenic uplift (West et al., 2005). Paleomagnetic data (Lippert et al., 2014; van Hinsbergen et al., 2012), tectonic models (Harrison et al., 1992), and sedimentary records from the Bengal Fan (Galy et al., 1996) all suggest that Indo-Asian continental lithosphere collision occurred between 25 and 20 Ma, causing widespread deformation of the Asian continent, exposing Greater Himalayan crystalline rocks to erosion. This increased exposure of fresh, unaltered silicate rock to weathering may have led to increased silicate weathering rates (and increased $F_{\text{Riv}}^{\text{Li}}$) at this time.

We compare our record of Li/Ca with records of other elements controlled (at least in part) by silicate weathering in Figure 5c. In general, as continental inputs to the oceans increase, the proportion of radiogenic ^{87}Sr (McArthur, 2004) and ^{187}Os (Burton et al., 2010; Ravizza & Peucker-Ehrenbrink, 2003) increases in seawater. The oceanic residence times of strontium and osmium are very different (respectively, >4 Myr and 10 kyr; Veizer, 1989; Oxburgh, 2001); hence, strontium is a proxy for multimillion year changes in silicate weathering fluxes, whereas osmium is controlled by short-term (sub-Myr) changes in weathering flux. The $^{87}\text{Sr}/^{86}\text{Sr}$ ratio of seawater can also be modified by carbonate weathering and/or episodes of intense volcanism (McArthur, 2004; Oliver et al., 2003), whereas $^{187}\text{Os}/^{188}\text{Os}$ is strongly influenced by inputs from black shales (Peucker-Ehrenbrink & Hannigan, 2000); therefore, caution is advised when using these proxies in isolation. Nevertheless, both strontium and osmium isotope data imply that continental inputs increased across the OMT (between 25 and 20 Ma; McArthur, 2004; Peucker-Ehrenbrink & Ravizza, 2000), although the $^{187}\text{Os}/^{188}\text{Os}$ record is interrupted by an abrupt decrease at the time of the Mi-1 oxygen isotopic excursion. Decreases in the $^{187}\text{Os}/^{188}\text{Os}$ composition of seawater are observed during many major glaciations and are attributed to a brief decrease in silicate weathering rates following global cooling, aridity, and ice sheet blanketing of silicate rocks (e.g., the Oi-1 and LGM; Burton et al., 2010; Oxburgh et al., 2007). Although data are limited, this transient decrease in the $^{187}\text{Os}/^{188}\text{Os}$ composition of seawater during Mi-1 is likely a result of a short interruption to the trend of increasing silicate weathering rates across the OMT caused by glacial inception (e.g., Lear et al., 2004). A significantly longer residence time means that this would not be apparent in Li/Ca records.

4.6. Changes in Organic Carbon Cycling During Mi-1

The increases we measure in planktonic foraminiferal $\delta^{13}\text{C}$ across the entire OMT and during the Mi-1 event suggest that thermocline $\delta^{13}\text{C}_{\text{DIC}}$ increased at this time. However, the close similarity of *D. venezuelana* values with $\delta^{13}\text{C}$ of benthic foraminifera suggests that thermocline $\delta^{13}\text{C}$ tracked the whole ocean increase in $\delta^{13}\text{C}_{\text{DIC}}$. Changes in thermocline $\delta^{13}\text{C}$ in response to enhanced primary productivity are generally more muted than they are in the surface mixed layer (Figure 2b). Hence, although this result gives further support for the hypothesized increase in organic carbon burial globally, *D. venezuelana* $\delta^{13}\text{C}$ alone does not provide evidence higher-surface water export production at Ceara Rise. By contrast, $\delta^{13}\text{C}$ values of *G. praebulloides* (Pearson et al., 1997), which inhabits the surface mixed layer, change by up to 1‰ at Site 926 during the Mi-1 event, reaching maxima at 22.95 and 23.02 Ma far in excess of modern surface water $\delta^{13}\text{C}_{\text{DIC}}$ at Ceara Rise ($>2.5\text{‰}$; Figure 1b). Furthermore, intervals of partial dissolution, such as that inferred from our shell weight records during Mi-1, are expected to artificially lower primary foraminiferal $\delta^{13}\text{C}$ (Lohmann, 1995). It is therefore

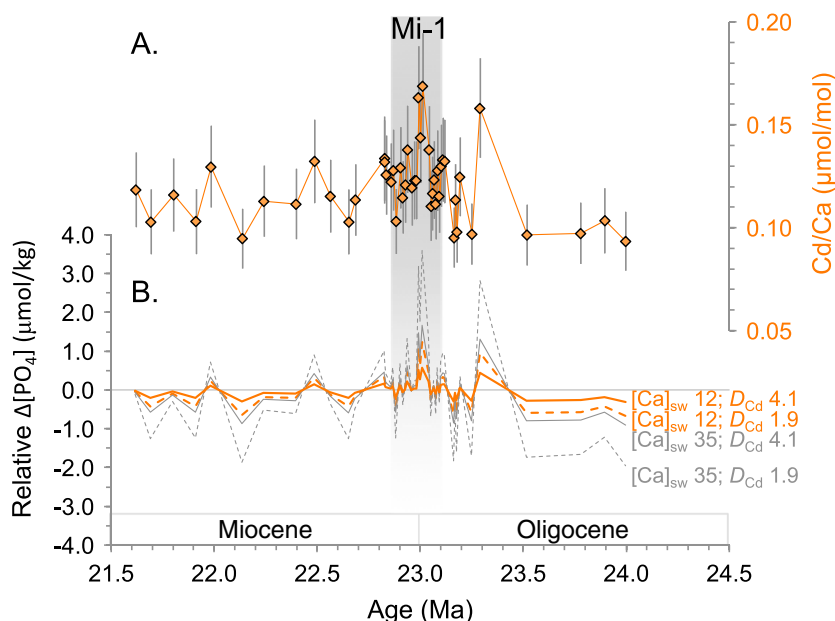


Figure 6. (a) Cd/Ca ratio of *D. venezuelana*. Gray bar represents the position of the Mi-1 event. (b) Relative change in thermocline $[\text{PO}_4]$ derived from foraminiferal Cd/Ca data, for various $[\text{Ca}]_{\text{sw}}$ and D_{Cd} values (see text for details).

likely that planktonic $\delta^{13}\text{C}$ values underestimate the increase in surface water $\delta^{13}\text{C}_{\text{DIC}}$ during the Mi-1. Changes in local weathering of shallow water carbonates, delivering ^{13}C -enriched carbon to surface waters, cannot be fully discounted during this interval of lower sea level (e.g., Merico et al., 2008). However, it is likely that the increases in surface water $\delta^{13}\text{C}_{\text{DIC}}$ during Mi-1 represent elevated primary production in surface waters that, in turn, may have increased export production at this site. This is supported by higher benthic foraminiferal mass accumulation rates during this interval, both at Ceara Rise and other sites in the South Atlantic (Figure 1c; Diester-Haass et al., 2011). Our data also support the idea that an increase in the ratio of organic carbon to carbonate burial acted to intensify this glacial expansion (Paul et al., 2000).

If primary test chemistry has been preserved (see section 4.2), then the Cd/Ca ratio of *D. venezuelana* can be used to reconstruct $[\text{PO}_4]$ in surface waters at Ceara Rise during the OMT using equation (2) (Figure 6). We assume that $(\text{Cd}/\text{P})_{\text{sw}}$ for equatorial Atlantic seawater is equal to the modern day value (0.25×10^{-3} ; de Baar et al., 1994), because benthic foraminiferal Cd/Ca shows little change across the Miocene (Delaney & Boyle, 1987). The effect of variable $(\text{Cd}/\text{P})_{\text{sw}}$ is small compared to the uncertainties in $[\text{Ca}]_{\text{sw}}$ and D_{Cd} (Figure 6b). Again, we assume values for $[\text{Ca}]_{\text{sw}}$ of 12 mmol/kg (Heuser et al., 2005) and 35 mmol/kg (Hardie, 1996) and D_{Cd} values between 1.9 and 4.1 (Delaney, 1989; Mashiotta et al., 1997). If the higher value for $[\text{Ca}]_{\text{sw}}$ is used, then thermocline $[\text{PO}_4]$ is between 4 and 10 $\mu\text{mol/kg}$, far higher than the concentrations found in modern deep waters at Ceara Rise ($[\text{PO}_4] < 1.5 \mu\text{mol/L}$) and even in upwelling regions ($[\text{PO}_4]$ up to 3.0 $\mu\text{mol/L}$; Garcia et al., 2010). If $[\text{Ca}]_{\text{sw}}$ is 12 mmol/kg, then estimated thermocline $[\text{PO}_4]$ values are more similar to those of the modern nutricline at Ceara Rise ($[\text{PO}_4] < 2.5 \mu\text{mol/L}$; Figure 2b; Garcia et al., 2010). The correspondence to modern values is even closer if D_{Cd} is 4.1 (calculated $[\text{PO}_4] \approx 1.5 \mu\text{mol/L}$) rather than 1.9 ($[\text{PO}_4] \approx 3 \mu\text{mol/L}$). Higher D_{Cd} values are common for subthermocline dwellers (e.g., *Gr. truncatulinoides*; Ripperger et al., 2008), and so this D_{Cd} value is arguably more applicable to the lower thermocline dwelling *D. venezuelana*. Hence, assuming $[\text{Ca}]_{\text{sw}} = 12 \text{ mmol/kg}$ and $D_{\text{Cd}} = 4.1$, we estimate that $[\text{PO}_4]$ increased by $\sim 0.5 \mu\text{mol/kg}$ during the Mi-1 event (Figure 6b). Although modest, this potentially equates to a shoaling of the nutricline at Ceara Rise by $\sim 100 \text{ m}$. This implies either (i) lower nutrient utilization or (ii) increased nutrient availability, at Ceara Rise during the Mi-1. The latter would support enhanced primary productivity. Neodymium isotope reconstructions of seawater during the OMT reveal the dominant influence of Amazon particulate material at Ceara Rise (Stewart et al., 2016). Changes in this local riverine flux of

weathered detrital material are therefore a clear candidate that could potentially alter the available surface dissolved phosphate at this site.

The U/Ca ratio of planktonic foraminifera is commonly used as a proxy for the carbonate saturation state of surface waters (Russell et al., 1996, 2004). However, foraminifera with high Mn/Ca ($>100 \mu\text{mol/mol}$), such as those analyzed in this study, tend to have elevated U/Ca ($>10 \text{ nmol/mol}$) that cannot represent a primary surface water signal (Lea et al., 2005; Mangini et al., 2001; Russell et al., 1996). All of our Ceara Rise samples have U/Ca values of $>40 \text{ nmol/mol}$ that are similar to values measured in benthic foraminifera at this site (Figure 1g; Mawbey & Lear, 2013). This suggests that the primary U/Ca signal has been modified during or after burial. Our U/Ca values can, however, provide information on the paleoredox state of sediments. If the concentration of dissolved oxygen is low in pore waters within sediments close to the sediment-seawater interface, then planktonic foraminiferal U/Ca values tend to be high (Algeo & Rowe, 2012; Lea et al., 2005; Russell et al., 1996). Thus, the increase in foraminiferal U/Ca measured in Site 926 OMT sediments represents a decrease in the oxygenation of sediment pore waters. This interpretation is consistent with the early termination of the U/Ca excursion ($\sim 100 \text{ kyr}$ before the termination of the Mi-1 event) that suggests postdepositional overprinting of U by authigenic carbonate (e.g., Thomson et al., 1995). Oxygen is utilized in the remineralization of organic matter, leading to lower oxygen in sediment pore waters during intervals of high organic carbon burial (Mangini et al., 2001; McManus et al., 2005; Russell et al., 1996). A decrease in pore water oxygen content during Mi-1 is therefore both consistent with our inferred increase in primary productivity, caused by increased nutrient availability at Ceara Rise, and it supports the hypothesis that respiratory dissolution is responsible for lower shell weight.

5. Conclusions and Wider Implications

Our high-resolution records of planktonic foraminiferal Li/Ca, Mg/Ca, Cd/Ca, U/Ca, $\delta^{18}\text{O}$, $\delta^{13}\text{C}$, and shell weight reveal that significant environmental changes occurred at Ceara Rise during the Mi-1 event. Increased Li/Ca during intervals of glacial intensification during the Mi-1, considered together with Mg/Ca and $\delta^{18}\text{O}$ data, reflects an increase in the carbonate saturation state of surface seawater. More work, however, is required to develop reliable core top/culture calibrations of Li/Ca versus Ω in modern planktonic foraminifera.

On longer ($>1 \text{ Ma}$) timescales, we observe an increase in Li/Ca in planktonic foraminiferal calcite from 24 to 21.5 Ma, which is interpreted to represent an increase in the lithium concentration in seawater caused by an increase in the riverine flux of lithium. This implies that rates of silicate weathering increased across the OMT, with uplift and erosion of the Himalaya and Tibetan Plateau providing a potential source of weatherable material. Increased silicate weathering may have triggered a period of extended drawdown of CO_2 and the initiation of widespread glacial expansion at 23 Ma (e.g., DeConto et al., 2008).

Increases in planktonic foraminiferal $\delta^{13}\text{C}$ and Cd/Ca during the Mi-1 event may be indicative of enhanced primary production boosted by greater nutrient supply to Ceara Rise surface waters during this interval. Evidence for an increase in organic carbon burial at this time is found in reduced oxygenation of sediment pore waters and an extended interval of respiratory dissolution of carbonates on the seafloor. Considered together, our findings suggest that while enhanced silicate weathering may have preconditioned the system for glaciation at this time, the majority of cooling at the Mi-1 (and hence rapid return to preexcursion global temperatures and glacial extent) was a result of drawdown of CO_2 caused by a short-lived increase in organic carbon burial rates.

References

- Algeo, T. J., & Rowe, H. (2012). Paleoclimatographic applications of trace-metal concentration data. *Chemical Geology*, 324–325, 6–18.
- Anand, P., Elderfield, H., & Conte, M. H. (2003). Calibration of Mg/Ca thermometry in planktonic foraminifera from a sediment trap time series. *Paleoceanography*, 18(2), 1050. <https://doi.org/10.1029/2002PA000846>
- Armstrong McKay, D. I., Tyrrell, T., & Wilson, P. A. (2016). Global carbon cycle perturbation across the Eocene-Oligocene climate transition. *Paleoceanography*, 31, 311–329. <https://doi.org/10.1002/2015PA002818>
- Arndt, S., Jørgensen, B. B., LaRowe, D. E., Middelburg, J. J., Pancost, R. D., & Regnier, P. (2013). Quantifying the degradation of organic matter in marine sediments: A review and synthesis. *Earth-Science Reviews*, 123, 53–86. <https://doi.org/10.1016/j.earscirev.2013.02.008>
- Bainbridge, A. (1980). *GEOSecs Atlantic ocean expedition*. Washington, DC: US Government Printing Office.
- Baker, P. A., Gieskes, J. M., & Elderfield, H. (1982). Diagenesis of carbonates in deep-sea sediments: Evidence from Sr/Ca ratios and interstitial dissolved Sr^{2+} data. *Journal of Sedimentary Research*, 52(1), 71–82.

Acknowledgments

This work used samples provided by the Ocean Drilling Program (ODP). The ODP (now IODP) is sponsored by the U.S. National Science Foundation and participating countries under management of the Joint Oceanographic Institutions (JOI), Inc. We thank Walter Hale and staff at the Bremen Core Repository for their help obtaining core material and also Guy Rothwell of BOSCORF for providing core top material for production of foraminiferal calcite standards. We are indebted to Kirsty Edgar, Clive Trueman, Gavin Foster, and Carrie Lear for their advice and helpful discussion of the manuscript; we also thank Megan Spencer, Bastian Hambach, Darryl Green, and Matt Cooper for their help with laboratory work. We thank Jim Zachos the reviewer and Ellen Thomas the Editor who provided constructive feedback that improved an earlier version of the manuscript. Data from this study can be found in the supporting information. We acknowledge financial support by the UK Natural Environment Research Council, award NE/D005108/1 (RHJ) and NE/K014137/1 (PAW) and a Royal Society Research Merit Award (PAW).

- Barker, S., & Elderfield, H. (2002). Foraminiferal calcification response to glacial-interglacial changes in atmospheric CO₂. *Science*, 297(5582), 833–836. <https://doi.org/10.1126/science.1072815>
- Beer, C. J., Schiebel, R., & Wilson, P. A. (2010a). Technical note: Determining the size-normalised weight of planktic foraminifera. *Biogeosciences Discussions*, 7(1), 905–920. <https://doi.org/10.5194/bgd-7-905-2010>
- Beer, C. J., Schiebel, R., & Wilson, P. A. (2010b). Testing planktic foraminiferal shell weight as a surface water [CO₃²⁻] proxy using plankton net samples. *Geology*, 38(2), 103–106. <https://doi.org/10.1130/G30150.1>
- Bemis, B. E., Spero, H. J., Bijma, J., & Lea, D. W. (1998). Reevaluation of the oxygen isotopic composition of planktonic foraminifera: Experimental results and revised paleotemperature equations. *Paleoceanography*, 13(2), 150–160. <https://doi.org/10.1029/98PA00070>
- Bemis, B. E., Spero, H. J., Lea, D. W., & Bijma, J. (2000). Temperature influence on the carbon isotopic composition of Globigerina Bulloides and Orbulina Universa (planktonic foraminifera). *Marine Micropaleontology*, 38(3–4), 213–228. [https://doi.org/10.1016/S0377-8398\(00\)00006-2](https://doi.org/10.1016/S0377-8398(00)00006-2)
- Boyle, E. A. (1981). Cadmium, zinc, copper, and barium in foraminifera tests. *Earth and Planetary Science Letters*, 53(1), 11–35. [https://doi.org/10.1016/0012-821X\(81\)90022-4](https://doi.org/10.1016/0012-821X(81)90022-4)
- Boyle, E. A., & Keigwin, L. D. (1985). Comparison of Atlantic and Pacific paleochemical records for the last 215,000 years: Changes in deep ocean circulation and chemical inventories. *Earth and Planetary Science Letters*, 76(1–2), 135–150. [https://doi.org/10.1016/0012-821X\(85\)90154-2](https://doi.org/10.1016/0012-821X(85)90154-2)
- Boyle, E. A., Sclater, F., & Edmond, J. M. (1976). On the marine geochemistry of cadmium. *Nature*, 263(5572), 42–44. <https://doi.org/10.1038/263042a0>
- Broecker, W. S., & Clark, E. (2001). Glacial-to-Holocene redistribution of carbonate ion in the deep sea. *Science*, 294(5549), 2152–2155. <https://doi.org/10.1126/science.1064171>
- Burton, K. W., Gannoun, A., & Parkinson, I. J. (2010). Climate driven glacial-interglacial variations in the osmium isotope composition of seawater recorded by planktic foraminifera. *Earth and Planetary Science Letters*, 295(1–2), 58–68. <https://doi.org/10.1016/j.epsl.2010.03.026>
- Burton, K. W., & Vance, D. (2000). Glacial-interglacial variations in the neodymium isotope composition of seawater in the Bay of Bengal recorded by planktonic foraminifera. *Earth and Planetary Science Letters*, 176(3–4), 425–441. [https://doi.org/10.1016/S0012-821X\(00\)00011-X](https://doi.org/10.1016/S0012-821X(00)00011-X)
- Channell, J. E. T., Galeotti, S., Martin, E. E., Billups, K., Scher, H. D., & Stoner, J. S. (2003). Eocene to Miocene magnetostratigraphy, biostratigraphy, and chemostratigraphy at ODP Site 1090 (sub-Antarctic South Atlantic). *Geological Society of America Bulletin*, 115(5), 607–623. [https://doi.org/10.1130/0016-7606\(2003\)115%3C0607:ETMMA%3E2.0.CO;2](https://doi.org/10.1130/0016-7606(2003)115%3C0607:ETMMA%3E2.0.CO;2)
- de Baar, H. J. W., Saager, P. M., Nolting, R. F., & van der Meer, J. (1994). Cadmium versus phosphate in the world ocean. *Marine Chemistry*, 46(3), 261–281. [https://doi.org/10.1016/0304-4203\(94\)90082-5](https://doi.org/10.1016/0304-4203(94)90082-5)
- DeConto, R. M., Pollard, D., Wilson, P. A., Pälike, H., Lear, C. H., & Pagani, M. (2008). Thresholds for Cenozoic bipolar glaciation. *Nature*, 455(7213), 652–656. <https://doi.org/10.1038/nature07337>
- Dekens, P. S., Lea, D. W., Pak, D. K., & Spero, H. J. (2002). Core top calibration of Mg/Ca in tropical foraminifera: Refining paleotemperature estimation. *Geochemistry, Geophysics, Geosystems*, 3(4), 1022. <https://doi.org/10.1029/2001GC000200>
- Delaney, M. L. (1989). Uptake of cadmium into calcite shells by planktonic foraminifera. *Chemical Geology*, 78(2), 159–165. [https://doi.org/10.1016/0009-2541\(89\)90114-9](https://doi.org/10.1016/0009-2541(89)90114-9)
- Delaney, M. L., Bé, A. W. H., & Boyle, E. A. (1985). Li, Sr, Mg, and Na in foraminiferal calcite shells from laboratory culture, sediment traps, and sediment cores. *Geochimica et Cosmochimica Acta*, 49(6), 1327–1341. [https://doi.org/10.1016/0016-7037\(85\)90284-4](https://doi.org/10.1016/0016-7037(85)90284-4)
- Delaney, M. L., & Boyle, E. A. (1987). Cd/Ca in late Miocene benthic foraminifera and changes in the global organic carbon budget. *Nature*, 330(6144), 156–159. <https://doi.org/10.1038/330156a0>
- Diester-Haass, L., Billups, K., & Emeis, K. (2011). Enhanced paleoproductivity across the Oligocene/Miocene boundary as evidenced by benthic foraminiferal accumulation rates. *Palaeogeography, Palaeoclimatology, Palaeoecology*, 302(3–4), 464–473. <https://doi.org/10.1016/j.palaeo.2011.02.006>
- Florindo, F., Gennari, R., Persico, D., Turco, E., Villa, G., Lurcock, P. C., ... Pekar, S. F. (2015). New magnetobiostratigraphic chronology and paleoceanographic changes across the Oligocene-Miocene boundary at DSDP Site 516 (Rio Grande Rise, SW Atlantic). *Paleoceanography*, 30, 659–681. <https://doi.org/10.1002/2014PA002734>
- Galy, A., France-Lanord, C., & Derry, L. A. (1996). The Late Oligocene-Early Miocene Himalayan belt constraints deduced from isotopic compositions of Early Miocene turbidites in the Bengal Fan. *Tectonophysics*, 260(1–3), 109–118. [https://doi.org/10.1016/0040-1951\(96\)00079-0](https://doi.org/10.1016/0040-1951(96)00079-0)
- Garcia, H. E., Locarnini, R. A., Boyer, T. P., Antonov, J. I., Zweng, M. M., Baranova, O. K., & Johnson, D. R. (2010). *World Ocean Atlas 2009, volume 4: Nutrients (phosphate, nitrate, silicate)*, NOAA Atlas NESDIS 71. Washington, DC: US Government Printing Office.
- Gasson, E., DeConto, R. M., Pollard, D., & Levy, R. H. (2016). Dynamic Antarctic ice sheet during the early to mid-Miocene. *Proceedings of the National Academy of Sciences*, 113(13), 3459–3464. <https://doi.org/10.1073/pnas.1516130113>
- Green, D. R. H., Cooper, M. J., German, C. R., & Wilson, P. A. (2003). Optimization of an inductively coupled plasma-optical emission spectrometry method for the rapid determination of high-precision Mg/Ca and Sr/Ca in foraminiferal calcite. *Geochemistry, Geophysics, Geosystems*, 4(6), 8404. <https://doi.org/10.1029/2002GC000488>
- Griffith, E. M., Paytan, A., Caldeira, K., Bullen, T. D., & Thomas, E. (2008). A dynamic marine calcium cycle during the past 28 million years. *Science*, 322(5908), 1671–1674. <https://doi.org/10.1126/science.1163614>
- Hain, M. P., Sigman, D. M., Higgins, J. A., & Haug, G. H. (2015). The effects of secular calcium and magnesium concentration changes on the thermodynamics of seawater acid/base chemistry: Implications for Eocene and Cretaceous ocean carbon chemistry and buffering. *Global Biogeochemical Cycles*, 29, 517–533. <https://doi.org/10.1002/2014GB004986>
- Hales, B., & Emerson, S. (1997). Calcite dissolution in sediments of the Ceara Rise: In situ measurements of porewater O₂, pH, and CO₂(aq). *Geochimica et Cosmochimica Acta*, 61(3), 501–514. [https://doi.org/10.1016/S0016-7037\(96\)00366-3](https://doi.org/10.1016/S0016-7037(96)00366-3)
- Hall, J. M., & Chan, L. H. (2004). Li/Ca in multiple species of benthic and planktonic foraminifera: Thermocline, latitudinal, and glacial-interglacial variation. *Geochimica et Cosmochimica Acta*, 68(3), 529–545. [https://doi.org/10.1016/S0016-7037\(03\)00451-4](https://doi.org/10.1016/S0016-7037(03)00451-4)
- Hall, J. M., Chan, L. H., McDonough, W. F., & Turekian, K. K. (2005). Determination of the lithium isotopic composition of planktic foraminifera and its application as a paleo-seawater proxy. *Marine Geology*, 217(3–4), 255–265. <https://doi.org/10.1016/j.margeo.2004.11.015>
- Hardie, L. A. (1996). Secular variation in seawater chemistry: An explanation for the coupled secular variation in the mineralogies of marine limestones and potash evaporites over the past 600 m.y. *Geology*, 24(3), 279–283. [https://doi.org/10.1130/0091-7613\(1996\)024%3C0279:SVISCA%3E2.3.CO;2](https://doi.org/10.1130/0091-7613(1996)024%3C0279:SVISCA%3E2.3.CO;2)
- Harrison, T. M., Copeland, P., Kidd, W. S. F., & Yin, A. N. (1992). Raising Tibet. *Science*, 255(5052), 1663–1670. <https://doi.org/10.1126/science.255.5052.1663>

- Hathorne, E. C., & James, R. H. (2006). Temporal record of lithium in seawater: A tracer for silicate weathering? *Earth and Planetary Science Letters*, 246(3-4), 393–406. <https://doi.org/10.1016/j.epsl.2006.04.020>
- Havach, S. M., Chandler, G. T., Wilson-Finelli, A., & Shaw, T. J. (2001). Experimental determination of trace element partition coefficients in cultured benthic foraminifera. *Geochimica et Cosmochimica Acta*, 65(8), 1277–1283. [https://doi.org/10.1016/S0016-7037\(00\)00563-9](https://doi.org/10.1016/S0016-7037(00)00563-9)
- Henson, S. A., Sanders, R., & Madsen, E. (2012). Global patterns in efficiency of particulate organic carbon export and transfer to the deep ocean. *Global Biogeochemical Cycles*, 26, GB1028. <https://doi.org/10.1029/2011GB004099>
- Heuser, A., Eisenhauer, A., Böhm, F., Wallmann, K., Gussone, N., Pearson, P. N., ... Dullo, W. C. (2005). Calcium isotope ($\delta^{44/40}\text{Ca}$) variations of Neogene planktonic foraminifera. *Paleoceanography*, 20, PA2013. <https://doi.org/10.1029/2004PA001048>
- Howarth, R. W. (1988). Nutrient limitation of net primary production in marine ecosystems, *Annual Review of Ecology and Systematics*, 19 (ArticleType: Research-article / Full publication date: 1988 / Copyright © 1988 Annual Reviews), 89–110.
- Huh, Y., Chan, L. H., Zhang, L., & Edmond, J. M. (1998). Lithium and its isotopes in major world rivers: Implications for weathering and the oceanic budget. *Geochimica et Cosmochimica Acta*, 62(12), 2039–2051. [https://doi.org/10.1016/S0016-7037\(98\)00126-4](https://doi.org/10.1016/S0016-7037(98)00126-4)
- Katz, A. (1973). The interaction of magnesium with calcite during crystal growth at 25–90°C and one atmosphere. *Geochimica et Cosmochimica Acta*, 37(6), 1563–1586. [https://doi.org/10.1016/0016-7037\(73\)90091-4](https://doi.org/10.1016/0016-7037(73)90091-4)
- Kisakürek, B., James, R. H., & Harris, N. B. W. (2005). Li and $\delta^7\text{Li}$ in Himalayan rivers: Proxies for silicate weathering? *Earth and Planetary Science Letters*, 237(3-4), 387–401. <https://doi.org/10.1016/j.epsl.2005.07.019>
- Kroopnick, P. M. (1985). The distribution of ^{13}C of ΣCO_2 in the world oceans. *Deep Sea Research Part A. Oceanographic Research Papers*, 32(1), 57–84. [https://doi.org/10.1016/0198-0149\(85\)90017-2](https://doi.org/10.1016/0198-0149(85)90017-2)
- Lea, D. W., Pak, D. K., & Paradis, G. (2005). Influence of volcanic shards on foraminiferal Mg/Ca in a core from the Galápagos region. *Geochemistry, Geophysics, Geosystems*, 6, Q11P04. <https://doi.org/10.1029/2005GC000970>
- Lea, D. W., Pak, D. K., & Spero, H. J. (2000). Climate impact of Late Quaternary Equatorial Pacific Sea surface temperature variations. *Science*, 289(5485), 1719–1724. <https://doi.org/10.1126/science.289.5485.1719>
- Lear, C. H., Elderfield, H., & Wilson, P. A. (2000). Cenozoic deep-sea temperatures and global ice volumes from Mg/Ca in benthic foraminiferal calcite. *Science*, 287(5451), 4.
- Lear, C. H., Rosenthal, Y., Coxall, H. K., & Wilson, P. A. (2004). Late Eocene to early Miocene ice sheet dynamics and the global carbon cycle. *Paleoceanography*, 19, PA4015. <https://doi.org/10.1029/2004PA001039>
- Liebrand, D., de Bakker, A. T., Beddow, H. M., Wilson, P. A., Bohaty, S. M., Ruessink, G., ... Lourens, L. J. (2017). Evolution of the early Antarctic ice ages. *Proceedings of the National Academy of Sciences*, 114(15), 3867–3872. <https://doi.org/10.1073/pnas.1615440114>
- Liebrand, D., Lourens, L. J., Hodell, D. A., de Boer, B., van de Wal, R. S. W., & Pälike, H. (2011). Antarctic ice sheet and oceanographic response to eccentricity forcing during the early Miocene. *Climate of the Past*, 7(3), 869–880. <https://doi.org/10.5194/cp-7-869-2011>
- Lippert, P. C., van Hinsbergen, D. J. J., & Dupont-Nivet, G. (2014). Early Cretaceous to present latitude of the central proto-Tibetan Plateau: A paleomagnetic synthesis with implications for Cenozoic tectonics, paleogeography, and climate of Asia. *Geological Society of America Special Papers*, 507. [https://doi.org/10.1130/2014.2507\(01\)](https://doi.org/10.1130/2014.2507(01))
- Locarnini, R. A., Mishonov, A. V., Antonov, J. I., Boyer, T. P., Garcia, H. E., Baranova, O. K., ... Seidov, D. (2013). In S. Levitus & A. Mishonov (Eds.), *World Ocean Atlas 2013, volume 1: Temperature*, NOAA Atlas NESDIS (Vol. 73, p. 40).
- Lohmann, G. P. (1995). A model for variation in the chemistry of planktonic foraminifera due to secondary calcification and selective dissolution. *Paleoceanography*, 10(3), 445–457. <https://doi.org/10.1029/95PA00059>
- Lorens, R. B. (1981). Sr, Cd, Mn and Co distribution coefficients in calcite as a function of calcite precipitation rate. *Geochimica et Cosmochimica Acta*, 45(4), 553–561. [https://doi.org/10.1016/0016-7037\(81\)90188-5](https://doi.org/10.1016/0016-7037(81)90188-5)
- Mangini, A., Jung, M., & Laukenmann, S. (2001). What do we learn from peaks of uranium and of manganese in deep sea sediments? *Marine Geology*, 177(1-2), 63–78. [https://doi.org/10.1016/S0025-3227\(01\)00124-4](https://doi.org/10.1016/S0025-3227(01)00124-4)
- Marriott, C. S., Henderson, G. M., Belshaw, N. S., & Tudhope, A. W. (2004). Temperature dependence of $\delta^7\text{Li}$, $\delta^{44}\text{Ca}$ and Li/Ca during growth of calcium carbonate. *Earth and Planetary Science Letters*, 222(2), 615–624. <https://doi.org/10.1016/j.epsl.2004.02.031>
- Marriott, C. S., Henderson, G. M., Crompton, R., Staubwasser, M., & Shaw, S. (2004). Effect of mineralogy, salinity, and temperature on Li/Ca and Li isotope composition of calcium carbonate. *Chemical Geology*, 212(1-2), 5–15. <https://doi.org/10.1016/j.chemgeo.2004.08.002>
- Mashiotto, T. A., Lea, D. W., & Spero, H. J. (1997). Experimental determination of cadmium uptake in shells of the planktonic foraminifera *Orbulina Universa* and *Globigerina Bulloides*: Implications for surface water paleoreconstructions. *Geochimica et Cosmochimica Acta*, 61(19), 4053–4065. [https://doi.org/10.1016/S0016-7037\(97\)00206-8](https://doi.org/10.1016/S0016-7037(97)00206-8)
- Mawbey, E. M., & Lear, C. H. (2013). Carbon cycle feedbacks during the Oligocene-Miocene transient glaciation. *Geology*, 41(9), 963–966. <https://doi.org/10.1130/G34422.1>
- McArthur, J. M. (2004). Sr-isotope stratigraphy: The Phanerozoic $^{87}\text{Sr}/^{86}\text{Sr}$ -curve and explanatory notes. In F. Gradstein, J. Ogg, & A. G. Smith (Eds.), *A Geological Timescale* (pp. 96–105). Cambridge, UK: Cambridge University Press.
- McCorkle, D. C., Martin, P. A., Lea, D. W., & Klinkhammer, G. P. (1995). Evidence of a dissolution effect on benthic foraminiferal shell chemistry: $\delta^{13}\text{C}$, Cd/Ca, Ba/Ca, and Sr/Ca results from the Ontong Java Plateau. *Paleoceanography*, 10(4), 699–714. <https://doi.org/10.1029/95PA01427>
- McManus, J., Berelson, W. M., Klinkhammer, G. P., Hammond, D. E., & Holm, C. (2005). Authigenic uranium: Relationship to oxygen penetration depth and organic carbon rain. *Geochimica et Cosmochimica Acta*, 69(1), 95–108. <https://doi.org/10.1016/j.gca.2004.06.023>
- Meece, D. E., & Benninger, L. K. (1993). The coprecipitation of Pu and other radionuclides with CaCO_3 . *Geochimica et Cosmochimica Acta*, 57(7), 1447–1458. [https://doi.org/10.1016/0016-7037\(93\)90005-H](https://doi.org/10.1016/0016-7037(93)90005-H)
- Merico, A., Tyrrell, T., & Wilson, P. A. (2008). Eocene/Oligocene ocean de-acidification linked to Antarctic glaciation by sea-level fall. *Nature*, 452(7190), 979–982. <https://doi.org/10.1038/nature06853>
- Miller, K. G., Wright, J. D., & Fairbanks, R. G. (1991). Unlocking the ice house: Oligocene-Miocene oxygen isotopes, eustasy, and margin erosion. *Journal of Geophysical Research*, 96(B4), 6829–6848. <https://doi.org/10.1029/90JB02015>
- Misra, S., & Froelich, P. N. (2012). Lithium isotope history of Cenozoic seawater: Changes in silicate weathering and reverse weathering. *Science*, 335(6070), 818–823. <https://doi.org/10.1126/science.1214697>
- Morozov, N. (1968). Geochemistry of rare alkaline elements in the oceans and seas. *Oceanology*, 8, 169–178.
- Oliver, L., Harris, N., Bickle, M., Chapman, H., Dise, N., & Horstwood, M. (2003). Silicate weathering rates decoupled from the $^{87}\text{Sr}/^{86}\text{Sr}$ ratio of the dissolved load during Himalayan erosion. *Chemical Geology*, 201(1-2), 119–139. [https://doi.org/10.1016/S0009-2541\(03\)00236-5](https://doi.org/10.1016/S0009-2541(03)00236-5)
- Oxburgh, R. (2001). Residence time of osmium in the oceans. *Geochemistry, Geophysics, Geosystems*, 2(6), 1018. <https://doi.org/10.1029/2000GC000104>
- Oxburgh, R., Pierson-Wickmann, A. C., Reisberg, L., & Hemming, S. (2007). Climate-correlated variations in seawater Os-187/Os-188 over the past 200,000 yr: Evidence from the Cariaco Basin, Venezuela. *Earth and Planetary Science Letters*, 263(3-4), 246–258. <https://doi.org/10.1016/j.epsl.2007.08.033>

- Pälike, H., Frazier, J., & Zachos, J. C. (2006). Extended orbitally forced palaeoclimatic records from the equatorial Atlantic Ceara Rise. *Quaternary Science Reviews*, 25(23-24), 3138–3149. <https://doi.org/10.1016/j.quascirev.2006.02.011>
- Pälike, H., Lyle, M. W., Nishi, H., Raffi, I., Ridgwell, A., Gamage, K., ... Zeebe, R. E. (2012). A Cenozoic record of the equatorial Pacific carbonate compensation depth. *Nature*, 488(7413), 609–614. <https://doi.org/10.1038/nature11360>
- Paul, H. A., Zachos, J. C., Flower, B. P., & Tripathi, A. (2000). Orbitally induced climate and geochemical variability across the Oligocene/Miocene boundary. *Paleoceanography*, 15(5), 471–485. <https://doi.org/10.1029/1999PA000443>
- Pearson, P. N., Shackleton, N. J., Weedon, G. P., & Hall, M. A. (1997). Multispecies planktonic foraminifera stable isotope stratigraphy through Oligocene/Miocene boundary climatic cycles, site 926. In N. J. Shackleton, et al. (Eds.), *Proceedings of the Ocean Drilling Program, Scientific Results* (Vol. 154, pp. 441–449). College Station, TX: Ocean Drilling Program.
- Peucker-Ehrenbrink, B., & Hannigan, R. E. (2000). Effects of black shale weathering on the mobility of rhenium and platinum group elements. *Geology*, 28(5), 475–478. [https://doi.org/10.1130/0091-7613\(2000\)28%3C475:EOBSWO%3E2.0.CO;2](https://doi.org/10.1130/0091-7613(2000)28%3C475:EOBSWO%3E2.0.CO;2)
- Peucker-Ehrenbrink, B., & Ravizza, G. (2000). The marine osmium isotope record. *Terra Nova*, 12(5), 205–219. <https://doi.org/10.1046/j.1365-3121.2000.00295.x>
- Ravizza, G., & Peucker-Ehrenbrink, B. (2003). The marine $^{187}\text{Os}/^{188}\text{Os}$ record of the Eocene-Oligocene transition: The interplay of weathering and glaciation. *Earth and Planetary Science Letters*, 210(1-2), 151–165. [https://doi.org/10.1016/S0012-821X\(03\)00137-7](https://doi.org/10.1016/S0012-821X(03)00137-7)
- Raymo, M. E., & Ruddiman, W. F. (1992). Tectonic forcing of late Cenozoic climate. *Nature*, 359(6391), 117–122. <https://doi.org/10.1038/359117a0>
- Rickaby, R. E. M., & Elderfield, H. (1999). Planktonic foraminiferal Cd/Ca: Paleonutrients or paleotemperature? *Paleoceanography*, 14(3), 293–303. <https://doi.org/10.1029/1999PA900007>
- Ripperger, S., Schiebel, R., Rehkämper, M., & Halliday, A. N. (2008). Cd/Ca ratios of in situ collected planktonic foraminiferal tests. *Paleoceanography*, 23, PA3209. <https://doi.org/10.1029/2007PA001524>
- Rosenthal, Y., Boyle, E. A., & Labeyrie, L. (1997). Last glacial maximum paleochemistry and deepwater circulation in the Southern Ocean: Evidence from foraminiferal cadmium. *Paleoceanography*, 12(6), 787–796. <https://doi.org/10.1029/97PA02508>
- Rosenthal, Y., Field, M. P., & Sherrell, R. M. (1999). Precise determination of element/calcium ratios in calcareous samples using sector field inductively coupled plasma mass spectrometry. *Analytical Chemistry*, 71(15), 3248–3253. <https://doi.org/10.1021/ac981410x>
- Rosenthal, Y., & Lohmann, G. P. (2002). Accurate estimation of sea surface temperatures using dissolution-corrected calibrations for Mg/Ca paleothermometry. *Paleoceanography*, 17(3), 1044. <https://doi.org/10.1029/2001PA000749>
- Rowley, D. B. (2002). Rate of plate creation and destruction: 180 Ma to present. *Geological Society of America Bulletin*, 114(8), 927–933. [https://doi.org/10.1130/0016-7606\(2002\)114%3C0927:ROPCAD%3E2.0.CO;2](https://doi.org/10.1130/0016-7606(2002)114%3C0927:ROPCAD%3E2.0.CO;2)
- Russell, A. D., Emerson, S., Mix, A. C., & Peterson, L. C. (1996). The use of foraminiferal uranium/calcium ratios as an indicator of changes in seawater uranium content. *Paleoceanography*, 11(6), 649–663. <https://doi.org/10.1029/96PA02058>
- Russell, A. D., Emerson, S., Nelson, B. K., Erez, J., & Lea, D. W. (1994). Uranium in foraminiferal calcite as a recorder of seawater uranium concentrations. *Geochimica et Cosmochimica Acta*, 58(2), 671–681. [https://doi.org/10.1016/0016-7037\(94\)90497-9](https://doi.org/10.1016/0016-7037(94)90497-9)
- Russell, A. D., Hönisch, B., Spero, H. J., & Lea, D. W. (2004). Effects of seawater carbonate ion concentration and temperature on shell U, Mg, and Sr in cultured planktonic foraminifera. *Geochimica et Cosmochimica Acta*, 68(21), 4347–4361. <https://doi.org/10.1016/j.gca.2004.03.013>
- Sexton, P. F., Wilson, P. A., & Pearson, P. N. (2006). Microstructural and geochemical perspectives on planktic foraminiferal preservation: "Glassy" versus "frosty". *Geochemistry, Geophysics, Geosystems*, 7, Q12P19. <https://doi.org/10.1029/2006GC001291>
- Shipboard Scientific Party (1995). Site 926. In W. B. Curry, et al. (Eds.), *Proceedings of the ocean drilling program. Initial reports* (Vol. 154, pp. 153–232). College Station, TX: Ocean Drilling Program.
- Smith, K. L., & Baldwin, R. J. (1984). Seasonal fluctuations in deep-sea sediment community oxygen consumption: Central and eastern North Pacific. *Nature*, 307(5952), 624–626. <https://doi.org/10.1038/307624a0>
- Stallard, R. F., & Edmond, J. M. (1983). Geochemistry of the Amazon 2. The influence of geology and weathering environment on the dissolved load. *Journal of Geophysical Research*, 88(C14), 9671–9688. <https://doi.org/10.1029/JC088C14p09671>
- Stewart, J. A., Gutjahr, M., James, R. H., Anand, P., & Wilson, P. A. (2016). Influence of the Amazon River on the Nd isotope composition of deep water in the western equatorial Atlantic during the Oligocene-Miocene transition. *Earth and Planetary Science Letters*, 454, 132–141. <https://doi.org/10.1016/j.epsl.2016.08.037>
- Stewart, J. A., Wilson, P. A., Edgar, K. M., Anand, P., & James, R. H. (2012). Geochemical assessment of the palaeoecology, ontogeny, morphotypic variability and palaeoceanographic utility of "Dentoglobigerina" venezuelana. *Marine Micropaleontology*, 84-85, 74–86. <https://doi.org/10.1016/j.marmicro.2011.11.003>
- Tachikawa, K., & Elderfield, H. (2002). Microhabitat effects on Cd/Ca and $\delta^{13}\text{C}$ of benthic foraminifera. *Earth and Planetary Science Letters*, 202(3-4), 607–624. [https://doi.org/10.1016/S0012-821X\(02\)00796-3](https://doi.org/10.1016/S0012-821X(02)00796-3)
- Takahashi, T., Broecker, W. S., & Bainbridge, A. E. (1981). The alkalinity and total carbon dioxide concentration in the world oceans. *Carbon cycle modelling, SCOPE*, 16, 271–286.
- Thomson, J., Higgs, N. C., Wilson, T. R. S., Croudace, I. W., De Lange, G. J., & Van Santvoort, P. J. M. (1995). Redistribution and geochemical behaviour of redox-sensitive elements around S1, the most recent eastern Mediterranean sapropel. *Geochimica et Cosmochimica Acta*, 59(17), 3487–3501. [https://doi.org/10.1016/0016-7037\(95\)00232-0](https://doi.org/10.1016/0016-7037(95)00232-0)
- Tyson, R. V. (2001). Sedimentation rate, dilution, preservation and total organic carbon: Some results of a modelling study. *Organic Geochemistry*, 32(2), 333–339. [https://doi.org/10.1016/S0146-6380\(00\)00161-3](https://doi.org/10.1016/S0146-6380(00)00161-3)
- van Hinsbergen, D. J. J., Lippert, P. C., Dupont-Nivet, G., McQuarrie, N., Doubrovine, P. V., Spakman, W., & Torsvik, T. H. (2012). Greater India Basin hypothesis and a two-stage Cenozoic collision between India and Asia. *Proceedings of the National Academy of Sciences*, 109(20), 7659–7664. <https://doi.org/10.1073/pnas.1117262109>
- Veizer, J. (1989). Strontium isotopes in seawater through time. *Annual Review of Earth and Planetary Sciences*, 17(1), 141–167. <https://doi.org/10.1146/annurev.ea.17.050189.001041>
- Vigier, N., Gislason, S. R., Burton, K. W., Millot, R., & Mokadem, F. (2009). The relationship between riverine lithium isotope composition and silicate weathering rates in Iceland. *Earth and Planetary Science Letters*, 287(3-4), 434–441. <https://doi.org/10.1016/j.epsl.2009.08.026>
- Walker, J. C. G., Hays, P. B., & Kasting, J. F. (1981). A negative feedback mechanism for the long-term stabilization of the Earth's surface temperature. *Journal of Geophysical Research*, 86(C10), 9776–9782. <https://doi.org/10.1029/JC086C10p09776>
- West, A. J., Galy, A., & Bickle, M. (2005). Tectonic and climatic controls on silicate weathering. *Earth and Planetary Science Letters*, 235(1-2), 211–228. <https://doi.org/10.1016/j.epsl.2005.03.020>
- Zachos, J. C., Shackleton, N. J., Revenaugh, J. S., Pälike, H., & Flower, B. P. (2001). Climate response to orbital forcing across the Oligocene-Miocene boundary. *Science*, 292(5515), 274–278. <https://doi.org/10.1126/science.1058288>